Macroscopic representation of structural geometry for simulating water and solute movement in dual-porosity media

Horst H. Gerke

*Department of Soil Landscape Research, Center for Agricultural Landscape and Land Use Research, Eberswalder Straße 84.
D-15374 Müncheberg, Germany*

&

Martinus Th. van Genuchten

*U.S. Salinity Laboratory, United States Department of Agriculture, Agriculture Research Service, 450 West Big Springs Road,
Riverside, California 92507-4617, USA*

The structure of *macroporous or* aggregated soils and fractured rocks is generally so complex that it is impractical to measure the geometry at the microscale (i.e., the size and the shape of soil aggregates or rock matrix blocks, and the myriad of fissures or fractures), and use such data in geometry-dependent macroscale flow and transport models. This paper analyzes a first-order type dual-porosity model which contains a geometry-dependent coefficient, β, in the mass transfer term to macroscopically represent the size and shape of soil or rock matrix blocks. As a reference, one- and two-dimensional geometry-based diffusion models were used to simulate mass transport into and out of porous blocks of defined shapes. Estimates for β *were* obtained analytically for four different matrix block geometries. Values for β were also calculated by directly matching analytical solutions of the diffusion models for a number of selected matrix block geometries to results obtained with the first-order model assuming standard boundary conditions. Direct matching improved previous results for cylindrical macropore geometries, especially when relatively small ratios between the outer soil mantle and the radius of the inner cylinder were used. Results of our analysis show that β is closely related to the ratio of the effective surface area available for mass transfer, and the soil matrix volume normalized by the effective characteristic length of the matrix system. Using values of β obtained by direct matching, an empirical function is derived to estimate macroscopic geometry coefficients from medium properties which in principle are measurable. The method permits independent estimates of β, thus allowing the dual-porosity approach eventually to be applied to media with complex and mixed types of structural geometry. Copyright © 1996 Published by Elsevier Science Ltd

Key *words:* preferential flow, variably-saturated structured media, dual-porosity model, mass transfer coefficient, geometry coefficient.

INTRODUCTION

Structured soils and fractured rock formations often contain macropores or fractures through which water and solutes can move at considerably larger velocities than in the porous matrix. The resulting microscopic or pore scale heterogeneities in flow velocities may eventually manifest themselves at the macroscopic scale in terms of preferential flow involving transient nonequilibrium conditions in the pressure head or solute concentration perpendicular to the flow direction. Preferential flow phenomena have been extensively studied[8,17,49] because of their implications on the hydrologic and contaminant transport properties of soil/rock systems. Dual- (or double-) porosity approaches[1,51] have been applied to various problems of water flow in fissured reservoirs, solute transport in aggregated soils, and transient flow and transport in variably-saturated structured media (for

an extensive review, see Gerke and van Genuchten[15]). Conceptually, a dual-porosity medium is generally assumed to involve two overlapping but interacting pore domains having different hydraulic and transport properties. Water and solute movement in dual-porosity models (e.g., Dykhuizen[13] and Jarvis *et al.*[24]) is simulated separately for the fracture and matrix pore systems, while coupling terms are used to describe the transfer of water and solutes between the two pore systems.

A commonality of dual-porosity approaches is that they require information about the geometry of the soil or rock system being simulated, i.e., the size and shape of matrix blocks or soil aggregates, including the geometry of the interface area through which water and solutes are exchanged between the two pore systems. The interface area may be associated with the surface structure of either the fracture pore system (e.g., planar cracks or cylindrical macropores), or of the matrix pore system itself (e.g., rock matrix blocks or soil aggregates). Naturally structured media often consist of a mixture of matrix blocks having different shapes and sizes, thereby leading to potentially very complex interfacial geometries as has been demonstrated recently by means of computed tomography.[20,25,50]

Mass transfer in dual-porosity models is frequently approximated using a first-order differential equation.[10,16,51] More sophisticated formulations that consider analytical solutions of flow and transport into or out of porous matrix blocks of known size and shape are generally limited to relatively simple situations, such as for well-defined macropore systems or idealized matrix block geometries,[34] steady-state water flow,[46] and for single pulses of water or solutes moving along a fracture.[14,52,53] Microstructure-type models[22,23,35,44] describing transport at both scales of the porous medium, i.e., macroscopic transport in the fracture pore system and local-scale transport inside the aggregates or matrix blocks, mostly assume a single equivalent matrix block geometry (e.g., a sphere) for which local-scale solutions of diffusion-type flow and transport models are available. Equivalent geometries may be obtained by deriving a volume-weighted average sphere radius,[32] using surface-to-volume ratios and distance probability functions for matrix diffusion obtained from fractured rocks or aggregated soils,[29,33] invoking scaling methods involving shape factors,[41,44] using scaling methods based on ratios between the volume and surface area of matrix blocks,[54] or by means of 'block -geometry functions' associated with planar, cylindrical, or spherical block shapes,[2] among other methods.

Although conceptually of considerable interest, the approaches above are still difficult to apply to field problems since the microscopic model parameters are not easily measured. A related issue, mostly still unresolved, is the question of how to obtain adequate microstructural information required to extend such models from simple or artificial media like glass beads to

field problems.' Consequently, the first-order mass transfer coefficient is at present still treated mostly as an empirical parameter which must be calibrated by fitting to observed field data, or to solute breakthrough curves obtained in displacement experiments.[45] One of the challenges of dual-porosity models is to identify those local-scale processes that have the most impact at the macroscale and to incorporate those processes in a macroscopic model in such a way that the model can be applied to realistic field problems. With respect to a structured dual-porosity medium, this means that the geometric effects somehow must be represented by a limited few lumped parameters related to the bulk volume of the medium. The aim of this paper is to derive expressions that appropriately describe the structural geometry of a dual-porosity medium using parameters that can be related to measurable properties.

DUAL-POROSITY MODEL AND FIRST-ORDER MASS TRANSFER

The dual-porosity model used in this study to simulate one-dimensional vertical water flow and solute transport in a variably-saturated structured medium was described in detail by Gerke and van Genuchten.[15] The model assumes that the properties of the bulk porous medium can be characterized by two sets of local-scale properties: one set associated with the fracture pore system (subscript f), and the other with the matrix pore system (subscript m), as follows

$$\epsilon = w_f \epsilon_f + (1 - w_f)\epsilon_m \tag{1a}$$

$$\theta = w_f \theta_f + (1 - w_f)\theta_m \tag{1b}$$

$$q = w_f q_f + (1 - w_f)q_m \tag{1c}$$

where ϵ is the porosity ($L^3 L^{-3}$), θ is the water content ($L^3 L^{-3}$), q is the fluid flux density (LT^{-1}), and w_f is the relative volumetric proportion of the fracture pore system ($0 \leq w_f \leq 1$). Assuming applicability of Darcy's law,[45] water flow in the fracture and matrix pore regions are described by a coupled pair of Richard's equations:

$$C_f \frac{\partial h_f}{\partial t} = \frac{\partial}{\partial z}\left(K_f \frac{\partial h_f}{\partial z} - K_f\right) - \frac{\Gamma_w}{w_f} \tag{2a}$$

$$C_m \frac{\partial h_m}{\partial t} = \frac{\partial}{\partial z}\left(K_m \frac{\partial h_m}{\partial z} - K_m\right) + \frac{\Gamma_w}{1 - w_f} \tag{2b}$$

where h is the pressure head (L), C is the specific water capacity $d\theta/dh$ (L^{-1}), K is the hydraulic conductivity (LT^{-1}), z is depth taken to be positive downward (L), t is time (T), and Γ_w is the water transfer term (T^{-1}) taken as

$$\Gamma_w = \alpha_w (h_f - h_m) \tag{3}$$

in which α_w is a first-order mass transfer coefficient

$(L^{-1}T^{-1})$ for water flow. The following expression for α_w was derived by Gerke and van Genuchten[16] using a scaling procedure:

$$\alpha_w = \frac{\beta}{a^2} \gamma_w K_a(h) \tag{4}$$

where β is a dimensionless geometry-dependent coefficient, a is the characteristic length of the matrix structure (L) (e.g., the radius of a spherical or solid cylindrical aggregate, or half the fracture spacing in the case of parallel rectangular voids), γ_w is a dimensionless scaling coefficient for which an average value of 0·4 was obtained empirically assuming parallel rectangular slabs (Fig. la), and K_a is the effective hydraulic conductivity function of the fracture-matrix interface evaluated in terms of both h_m and h_f as follows

$$K_a = 0·5[K_a(h_f) + K_a(h_m)] \tag{5}$$

Analogous to eqn (2), the transport of solutes in a variably-saturated dual-porosity medium is described using two coupled convection-dispersion equations:

$$\frac{\partial}{\partial t}(\theta_f R_f c_f) = \frac{\partial}{\partial z}\left(\theta_f D_f \frac{\partial c_f}{\partial z} - q_f c_f\right) - \frac{\Gamma_s}{w_f} \tag{6a}$$

$$\frac{\partial}{\partial t}(\theta_m R_m c_m) = \frac{\partial}{\partial z}\left(\theta_m D_m \frac{\partial c_m}{\partial z} - q_m c_m\right) + \frac{\Gamma_s}{1 - w_f} \tag{6b}$$

where D is the dispersion coefficient $(L^2 T^{-1})$, R is a dimensionless retardation factor accounting for linear equilibrium sorption, and Γ_s is the solute mass transfer term $(ML^{-3}T^{-1})$ formulated here in a slightly different way as done previously in Gerke and van Genuchten."

$$\Gamma_s = \alpha_s(1 - w_f)\theta_m(c_f - c_m) + \begin{cases} \Gamma_w c_f & \Gamma_w \geq 0 \\ \Gamma_w c_m & \Gamma_w < 0 \end{cases} \tag{7}$$

in which α_s is the first-order solute mass transfer coefficient (T^{-1}) of the form

$$\alpha_s = \frac{\beta}{a^2} D_a \tag{8}$$

where D_a is an effective diffusion coefficient $(L^2 T^{-1})$ which represents the diffusion properties of the fracture-matrix interface as well as other parameters and which, however, has not yet been evaluated analogously to $\gamma_w K_a$ in eqn (4) for water transfer.

For steady-state water flow with $q_m = 0$ (no flow in the matrix pore system), the above variably-saturated dual-porosity model reduces to the two-region mobile-immobile solute transport model of van Genuchten and Wierenga.[43]

$$\vartheta_f R_f^* \frac{\partial c_f}{\partial t} + \vartheta_m R_m^* \frac{\partial c_m}{\partial t} = \vartheta_f D_f \frac{\partial^2 c_f}{\partial z^2} - \vartheta_f \nu_f \frac{\partial c_f}{\partial z} \tag{9a}$$

$$\vartheta_m R_m^* \frac{\partial c_m}{\partial t} = \alpha_s^*(c_f - c_m) \tag{9b}$$

where the water contents, ϑ_f and ϑ_m, as well as the retardation factors, R_f^* and R_m^*, are expressed in terms of

the bulk soil volume, i.e.,

$$\vartheta_f = w_f \theta_f; \qquad \vartheta_m = (1 - w_f)\theta_m \tag{10a; b}$$

The first-order mass transfer coefficient, $\alpha_s^*(T^{-1})$, in (9b) characterizing diffusive exchange of solutes between the mobile and immobile liquid phases is of the general form

$$\alpha_s^* = \frac{\beta \vartheta_m D_m^*}{a^2} \tag{11}$$

where D_m^* is the effective diffusion coefficient for solute mass transfer into the immobile pore water region or the matrix pore system. We refer to Gerke and van Genuchten" and van Genuchten[42] for additional discussions of the dual-porosity models presented here, including possible ways of how the different parameters, other than β, may be measured or estimated.

GEOMETRY REPRESENTATION OF THE MASS TRANSFER COEFFICIENT

Analytical evaluation

In order to relate the mass transfer coefficient, α_s^*, to the diffusion properties of soil aggregates or rock matrix blocks, the first-order formulation given by eqns (9) and (11) may be compared with more comprehensive geometry-based microstructure-type models for diffusion into porous blocks having spherical, cylindrical, or rectangular slab-type geometries. A variety of techniques have been used to derive expressions for α_s^* in eqn (11), including Laplace transform comparisons,[31,39,44] moment analysis,[30,40] and the use of algebraic expansions.[4] The Laplace transform method may also be used to derive expressions for the first-order water transfer coefficient, α_w, in eqn (4) by linearizing the horizontal flow equation.[16] Such analyses lead to first-order mass transfer coefficients in eqns (4), (8), and (11) which are of the general form

$$\alpha_w \equiv \alpha_s \equiv \frac{\alpha_s^*}{\vartheta_m} = \frac{\beta}{a^2} P \tag{12}$$

with $P = D_m^*$ in the two-region mobile-immobile type transport model (9), D_a in the dual-porosity solute transport model (6), and $\gamma_w K_a$ in the dual-porosity water flow model (2). Thus, we hypothesize that values of β can be derived that are identical for these three models, and hence a function only of the geometry.

Mass transfer coefficients obtained analytically using Laplace transform comparisons differ only in the value of the geometry-dependent coefficient, β. Most of the studies mentioned above derived values for β of 3 for rectangular slabs, 8 for solid cylinders, and 15 for spheres, although other studies obtained slightly different values.[13,38] For a hollow cylindrical dual-porosity medium involving macropores surrounded by cylindrical soil or rock matrix mantles, van Genuchten and

Dalton[44] derived the following expression for β:

$$\beta = \frac{2(\zeta_0 - 1)^2}{\zeta_0^2[\ln(\zeta_0) - 1]}; \qquad \zeta_0 \gg 1 \qquad (13)$$

where $\zeta_0 = (a + b)/b$, in which b is the radius of the cylindrical macropore and a is the thickness of the soil matrix mantle (Fig. 1b).

For hollow cylindrical geometries the flux across the fracture-matrix interface (the surface of the inner cylinder) is very similar to the soil water flux into a root located in the center of a cylindrical soil segment.

The latter process has been widely studied.[28] Analogous to the water transfer term, Γ_w, root water uptake is generally included as a sink term in the Richard's equation (2), and often formulated as an effective first-order approach. Such an approach was actually used by Moldrup *et al.*[27] who derived a soil resistance term by integrating the flow equation for a cylindrical coordinate system between the inner and outer radius of the soil mantle and assuming $d\theta/dt$ to be constant ($>O$). This approach leads to another equivalent expression for the geometry-dependent coefficient, β. Using the notation of this paper, this alternative expression is
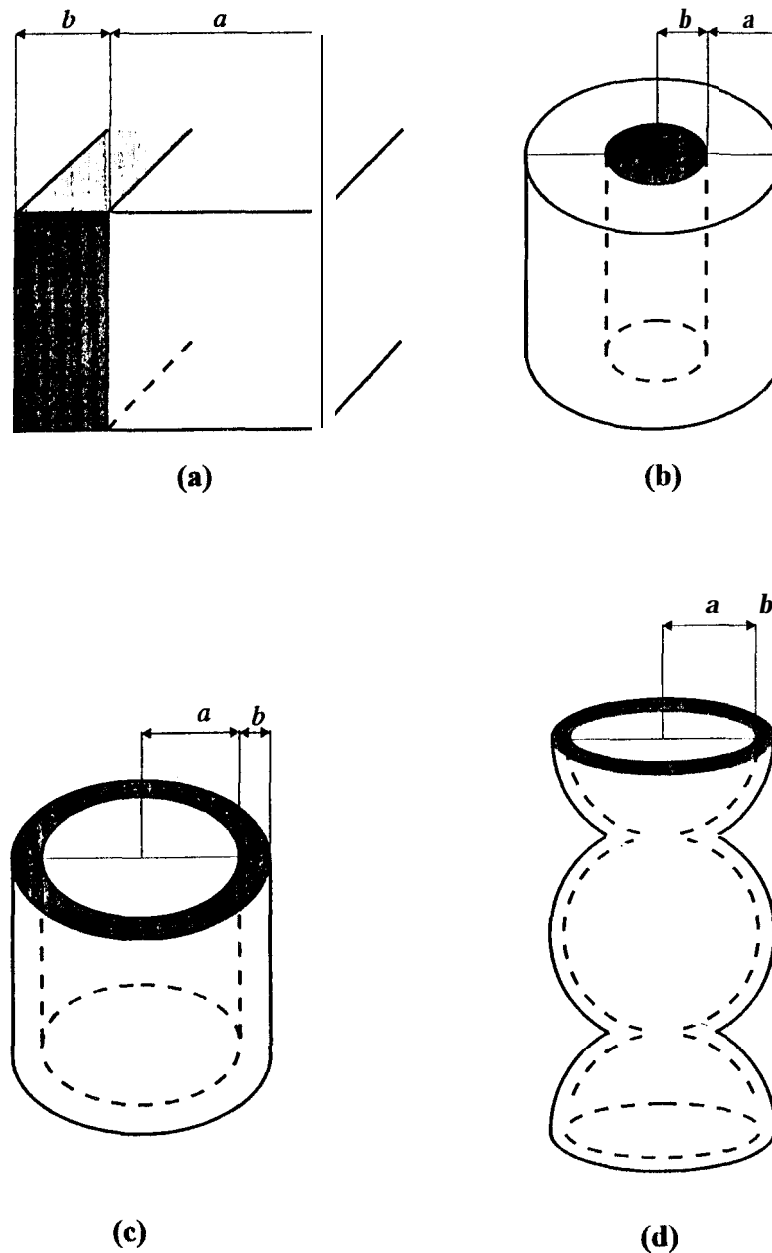

(a)

(b)

(c)

(d)

Fig. 1. Schematic illustration of porous blocks having (a) rectangular slab-type, (b) hollow cylindrical, (c) solid cylindrical, and (d) spherical geometries. Widths of *2a* and *2b* are associated with the matrix and fracture pore systems, respectively.

given by

$$\beta = \left[\ln(\zeta_0) \cdot \frac{\zeta_0^2}{\zeta_0^2 = 1} - 0.5 \right]^{-1} ; \quad \zeta_0 > 1 \qquad (14)$$

Analytically derived mass transfer coefficients are limited to basically four geometries for which solutions of the diffusion equations are available. Additional limitations are due to simplifying assumptions made during mathematical derivation of the coefficients, e.g., neglecting higher-order terms in the series expansions.

Direct **matching**

Alternatively, estimates for the mass transfer coefficient, α_s^*, may also be obtained by directly matching solutions of the first-order approach, i.e., of eqn (9b), with calculated average solute concentrations of soil aggregates or rock matrix blocks of known geometry. For this purpose one could use analytical solutions of the equations governing diffusion into spherical, rectangular (slab-type), or solid cylindrical aggregates, or those pertaining to diffusion from hollow cylindrical macropores into the surrounding soil matrix. The direct matching technique was previously used by van Genuchten[41] to compare the diffusion properties of a soil aggregate with given geometry and size with those having different shapes and sizes in a nonflowing system. His method is employed here to obtain geometry-dependent coefficients for various matrix block sizes for use in the first-order transfer terms. The direct matching technique is demonstrated below for the case of a hollow cylindrical macropore geometry.

Radial diffusion from the macropore through the surface of the inner cylinder (Fig. lb) into the surrounding mantle (assuming an infinite longitudinal length) is described by

$$R_m^* \frac{\partial c_a}{\partial t} = \frac{D_m^*}{r} \frac{\partial}{\partial r} \left(r \frac{\partial c_a}{\partial r} \right) \qquad b \leq r \leq (a+b) \qquad (15)$$

where $c_a(r,t)$ is the local solute concentration inside the cylindrical soil mantle, r is the local radial coordinate, and the subscript m indicates that R_m^* and D_m^* represent matrix pore system properties which are consistent with the transport model in eqn (9) at the macroscopic scale. We assume here that the solute concentration of the matrix pore system, c_m, defines the average solute concentration, $\bar{c}_a$, of the liquid phase in the hollow cylindrical (subscript h) porous matrix as follows

$$\bar{c}_a(t) = \frac{2}{(a+b)^2 - b^2} \int_b^{a+b} r\, c_a(r,t)\, dr \qquad (16)$$

in which a is the characteristic length (the radial width of

the soil mantle surrounding the macropore). Solving eqn (15) for a uniform initial solute concentration, $c_a(r, 0)$, of zero, a constant concentration of unity at the inner, $c_a(b, t) = 1$, and a zero concentration gradient (no flow) at the outer boundary (at $r = a + b$), and substituting that solution into eqn (16) leads to[9]

$$\bar{c}_a(\tau_h) = 1 - \frac{2\pi}{\zeta_0^2 - 1} \sum_{n=1}^{\infty}$$

$$\times \frac{J_1^2(\mu_n \zeta_0 [J_0(\mu_n) Y_1(\mu_n) - J_1(\mu_n) Y_0(\mu_n)]}{\mu_n [J_1^2(\mu_n \zeta_0) - J_0^2(\mu_n)]}$$

$$\times \exp(-\mu_n^2 \tau_h) \qquad (17)$$

where J_0, J_1, Y_0, and Y_1 are Bessel functions and μ_n are positive roots of

$$J_0(\mu_n) Y_1(\mu_n \zeta_0) - J_1(\mu_n \zeta_0) Y_0(\mu_n) = 0 \qquad (18)$$

and where $\bar{c}_a$ is expressed in terms of dimensionless time, τ_h, as follows

$$\tau_h = \frac{D_m^* t}{R_m^* a_h^2} \qquad (19)$$

and where the subscript h on τ and a is used to indicate a hollow cylindrical macropore.

Analogously, solutions for the average concentrations, $\bar{c}_a$, as a function of dimensionless time, τ, are available for spherical, solid cylindrical, and rectangular geometries.[9,11] Plots of the resulting curves of $\bar{c}_a(\tau)$ versus τ for different aggregate geometries exhibit relatively similar, but not identical, sigmoidal shapes.[41] In the original paper, van Genuchten[41] introduced a 'shape factor', f, for conversion of one geometry into an equivalent other geometry by matching the $F_{,(\tau)}$ curves of two geometries through modification of the characteristic length a in the dimensionless time (e.g., eqn (19)) pertaining to one of those geometries. The shape factor was evaluated at an average value of $\bar{c}_a = 0.5$, thus ignoring any observed dependency off on $\bar{c}_a$.

A similar approach can be used for estimating shape factors in the first-order transfer term.[41] Integrating eqn (9b) for $c,(0) = 0$ and $c_f(t) = 1$ gives

$$\bar{c}_a \equiv c_m(\tau_0) = 1 - \exp(-\tau_0) \qquad (20)$$

where

$$\tau_0 = \frac{\alpha_s^* t}{\vartheta_m R_m^*} \qquad (21)$$

is the dimensionless time in the first-order model (subscript 0). The shape factor $f_{h,0}$ for converting a hollow cylindrical into the equivalent first-order rate model was defined by van Genuchten[41] as

$$f_{h,0} = \left(\frac{\tau_h}{\tau_0} \right)^{1/2} \Bigg|_{\bar{c}_a = 0.5} \qquad (22)$$

in which the dimensionless times τ_h and τ_0 were both evaluated at $\bar{c}_a = c_m = 0.5$. Substituting eqns (19) and

(21) into eqn (22) shows that the shape factor,f, is related to the geometry coefficient, β, in the first-order transfer term of the dual-porosity model by means of $\beta = 1/f^2$.

By using the direct matching method, we obtained values for β of 3·5 for rectangular slabs, 11 for solid cylinders, 22·7 for spheres (see also van Genuchten[41]), and the following empirical regression function ($r^2 = 0.996$) for a hollow cylindrical geometry:

$$\beta = \frac{1}{[0·19 \ln(16\zeta_0)]^2}; \qquad 1 < \zeta_0 < 100 \qquad (23)$$

Figure 2 compares the geometry coefficients for hollow cylindrical matrix geometries as obtained by means of analytical derivation (eqns (13) and (14)) with those obtained using eqn (23) which is based on the direct matching approach. Equation (13) closely agrees with the direct matching results in the limit of relatively thick cylindrical soil mantles (large ζ_0), whereas eqn (14) approximates the direct matching results more closely in the limit when $\zeta_0 \rightarrow 1$. The results in Fig. 2 are a consequence of simplifying assumptions invoked in the derivations of eqns (13) and (14), i.e., by having systems with relatively few macropores per unit area ($\zeta_0 > 10$), or relatively dense root systems ($\zeta_0 < 5$). The effect of using different values of β in eqn (4) on soil water flow

simulations will be shown later by directly comparing the dual-porosity model with equivalent two-dimensional models for different matrix geometries. We note that the scaling procedure described by Gerke and van Genuchten[16] was employed to evaluate the hydraulic conductivity of the fracture-matrix interface, $K_a(h)$, in eqn (4) using the analytically-derived geometry coefficient for parallel rectangular slabs ($\beta = 3$).

COMPARISONS USING EQUIVALENT TWO-DIMENSIONAL MODELS

To study the geometry coefficients in the mass transfer term (4) as evaluated by different methods, consider transient unsaturated water flow in both the fracture and matrix pore systems. For convenience, and to facilitate a direct comparison, vertical movement in the matrix pore system has been neglected. Results obtained with the dual-porosity model using the first-order transfer term will be compared with those generated using the SWMS_2D finite element code." The flow region was designed to imitate rectangular, hollow cylindrical, and solid cylindrical geometries of the matrix blocks (Fig. 1). Hydraulic properties of relatively
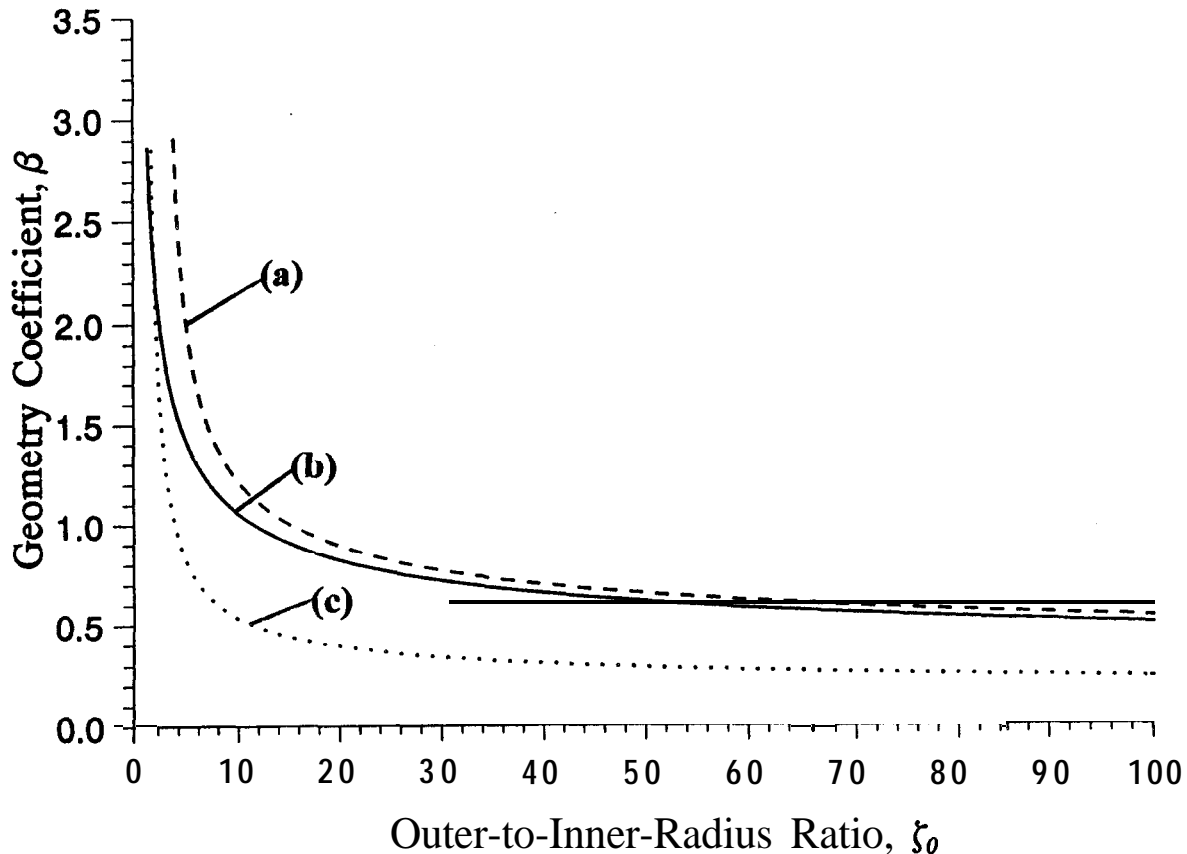

Fig. 2. The geometry coefficient, β, as a function of the ratio, ζ_0, between the outer and inner radius, assuming hollow cylindrical geometry. Plotted are values and curves obtained by (a) analytical derivation using eqn (13), (b) direct matching using eqn (23), and (c) analytical derivation using eqn (14).

Table 1. Model parameters and initial conditions used in the twodimensional comparisons

	α (1/cm)	n	θ_r	θ_s	K_s (cm/day)	$h_i(z)$ (cm)	$\theta_i(z)$
Matrix	0·005	1.5	0.11	0·5	1·05	−1000	0·277
Fracture	0.100	2·0	0·0	0·5	2000	-1000	0·005

coarse- and fine-textured soil materials (Table 1) were assigned to the fracture and matrix pore systems, respectively. Water flow for the parallel rectangular fracture (slab) geometry was simulated by using a two-dimensional cross-section (x-z plane) where x is the horizontal and z is the vertical spatial direction. For cylindrical geometries we assumed radial symmetry, and simulated flow in a quasi three-dimensional region *(r-z* plane) using the flow equation for a cylindrical coordinate system. In order to compare the results of the two-dimensional calculations with those obtained with the dual-porosity model (2), nodal water contents at given simulation times were averaged over the horizontal or radial distance and transformed into equivalent pressure head values of the fracture and matrix pore systems using the inverse of the water retention function (e.g., van Genuchten *et al.*[47]):

$$h = \frac{1}{\alpha}\left(S_e^{-1/m} - 1\right)^{1/n} \qquad (24)$$

where α and *n* are empirical parameters, $m = 1 - 1/n$, $S_e = (\theta - \theta_r)/(\theta_s - \theta_r)$ is effective saturation, and θ_r and θ_s are the residual and saturated water contents, respectively. The procedure used for comparing modeling results is described in detail by Gerke and van Genuchten.[16]

For the idealized geometries (Fig. 1) used here, the characteristic length, *b* (e.g., the half-width in the case of a rectangular slab, or the radius in the case of a cylinder or sphere) of the fracture pore system is related to the relative proportion of the fracture system, w_f, and the characteristic length, *a,* of the matrix system by

$$B_l = a_l \frac{w_f}{1 - w_f} \qquad (25)$$

for rectangular slabs (subscript l), by

$$b_h = a_h \frac{(w_f)^{1/2}}{1 - (w_f)^{1/2}} \qquad (26)$$

for hollow cylinders (subscript h), and by

$$b_{c;r} = a_{c;r}[(1 - w_f)^{-1/2} - 1] \qquad (27)$$

for solid cylinders (subscript c); for rectangular prisms (subscript r) we assumed a square base area of $(2a)^2$. Flow systems containing a spherical geometry were approximated by assuming that the spherical matrix blocks or soil aggregates were surrounded by thin spherical mantles imitating the fracture pore system. In case the spheres are completely surrounded by the fractures, the equivalent characteristic length of the fracture system, b_s^*, is

$$b_s^* = a_s[(1 - w_f)^{-1/3} - 1] \qquad (28)$$

Assuming that the spherical matrix blocks are in contact with each other (Fig. Id), the volume, V_{sc}, of the top and bottom sphere-caps (subscript SC) of the fracture mantle

$$V_{sc} = \frac{\pi}{3} b_s^2 (3a_s + 2b_s) \qquad (29)$$

has to be distributed in the fracture pore system resulting in a value of b_s which is slightly larger than b_s^* as follows

$$b_s^3 - 3a_s \frac{0.5 - w_f}{w_f} b_s^2 - 3a_s^2 \frac{1 - w_f}{w_f} b_s + a_s^3 = 0 \qquad (30)$$

Equation (30) can either be solved exactly, using a closed-form trigonometric solution for cubic equations, or solved approximately in an iterative manner beginning with b_s^* obtained from eqn (28) as the initial estimate. For example, assuming $a = 1$ cm and $w_f = 0.05$, one obtains $b_s^* = 0.017245$ cm and $b_s \approx 0.0174$ cm. The values of *b* for the other geometries (Table 2) were used to design equivalent two-dimensional flow regions and associated numerical finite element discretizations.

To illustrate physical nonequilibrium during transient flow in an unsaturated dual-porosity-type structured porous medium, the simulation example used previously[15,16] was selected. We assumed the application of water at a constant rate of 50 cm/day to a 40-cm-deep dual-porosity medium having an initial uniform pressure head of $h_{f,i} = h_{m,i} = -1000$ cm. Water was allowed to infiltrate exclusively into the fracture pore system ($w_f = 0.05$), such that a local infiltration rate of $q_{f,0} = 1000$ cm/day was imposed at the upper and a free-drainage condition at the lower boundary of the

Table 2. Model parameters in first-order transfer term and two-dimensional representation

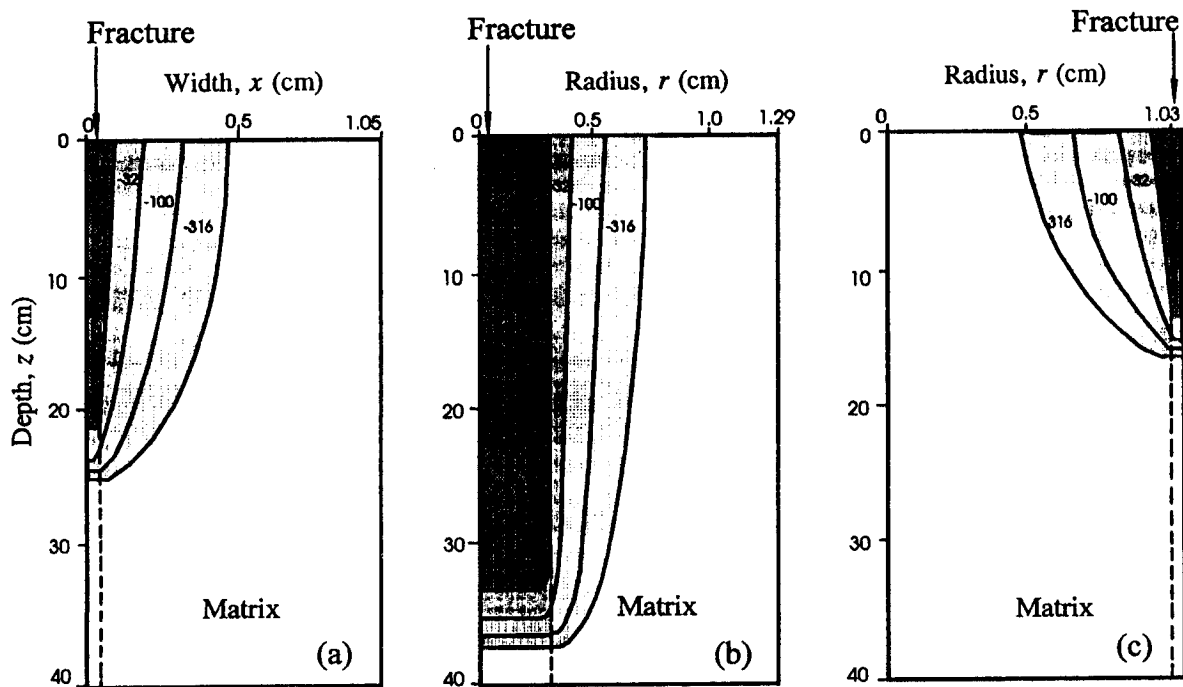|	β analytic	β matching	a (cm)	b (cm)	γ_w	$K_{s,a}$ (cm/day)	
Rectangular slab	3	3·5	1	0.02563	0·4	0.01	0·1
Solid cylinder	8	11·0	1	0.02598	0·4	0·01	0·1
Hollow cylinder	2.42	1·5	1	0.28800	0·4	0.01	0·1

Fig. 3. Pressure head distribution in vertically layered fracture/matrix profiles assuming (a) rectangular slab-type, (b) hollow cylinder, and (c) solid cylinder fracture or matrix geometries, and obtained with (a) two-dimensional, (b) and (c) three-dimensional axisymmetric flow model, at $t = 0.04$ days. The profile height is 40 cm; the horizontal, x, and radial, r, axes are enlarged 20 times.
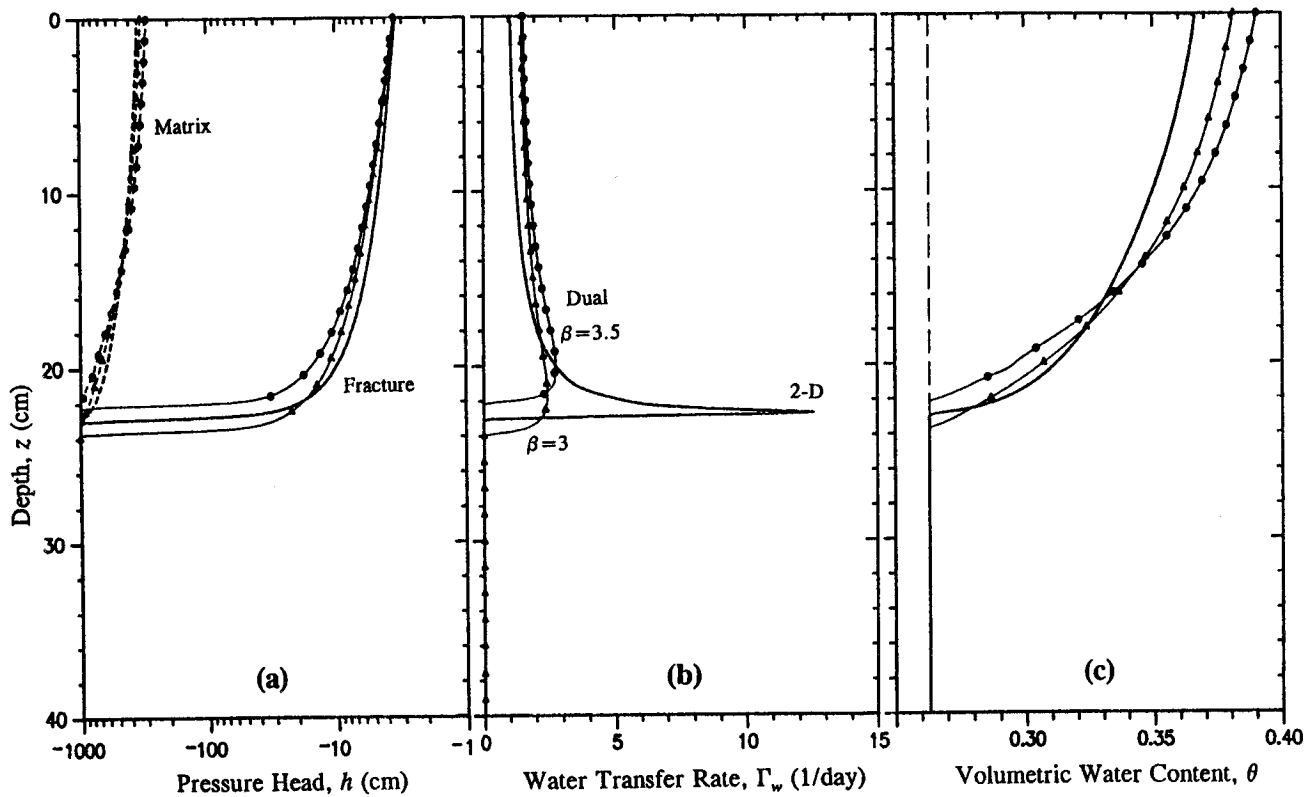

Fig. 4. Pressure head, h (a), water transfer rate, Γ_w (b), and total volumetric water content, θ (c), versus depth, z, at $t = 0.04$ days as calculated with the one-dimensional dual-porosity (Dual) and two-dimensional (2-D) models, assuming a rectangular slab-type geometry and relatively small water transfer rates ($K_{s,a} = 0.01$ cm/day); results are for geometry coefficients derived analytically ($\beta = 3$) and by direct matching ($\beta = 3.5$).

fracture pore system. Parameters of the soil water retention function $(\alpha, n, \theta_r, \theta_s)$, the hydraulic conductivity at saturation, K_s, the initial pressure head, h_i, and water content, θ_i, and the first-order mass transfer coefficients can be found in Tables 1 and 2, respectively.

Figure 3 shows calculated two-dimensional pressure head distributions at $t = 0.04$ days for (a) a parallel rectangular slab, (b) a hollow cylindrical geometry, and (c) a solid cylindrical geometry assuming relatively low $(K_{s,a} = 0.01$ cm/day) water transfer rates between the fracture and matrix pore systems. Note that the horizontal axis is enlarged 20 times. The simulation examples in Fig. 3 illustrate significant preferential flow and pressure head nonequilibrium between the fracture and matrix pore domains for all three geometries. After about 1 hour ($t = 0.04$ days) of constant infiltration, water moved downward to a depth of 23cm in the rectangular pore system (Fig. 3a), to z = 35 cm in the hollow cylindrical pore system (Fig. 3b), and to z = 15cm in the fracture pore system surrounding the solid cylindrical soil matrix (Fig. 3c). Since all model parameters, including the relative volume, w_f, of the fracture pore system and the initial and boundary conditions were identical, differences in calculated pressure distributions were caused only by the geometry-dependent rates of water transfer from the fracture into the matrix pore system. Two-dimensional model simulations were also carried out for the case of relatively high water transfer rates assuming $K_{s,a} = 0.1$ cm/day (results not shown here).

Horizontally averaged two-dimensional simulation results are compared with results obtained from the dual-porosity model for relatively small water transfer rates ($K_{s,a} = 0.0$ 1 cm/day) assuming matrix structures involving rectangular slabs (Fig. 4), hollow cylinders (Fig. 5), and solid cylinders (Fig. 6). As was discussed previously,[16] the first-order term generally underestimates the transfer rate at the infiltration front due to failure of the linear first-order term to capture the highly nonlinear transient flow process near the front (see also Zimmerman *et al.*[55]). However, except in areas close to the infiltration front, the proposed linear term yielded relatively good approximations for the transfer of water (parts b of Figs 4–7), so that the calculated pressure head (parts a) and water content profiles (parts c) still closely matched the reference results. The match generally improved when allowing higher water transfer rates by using $K_{s,a} = 0.1$ cm/day (*cf.*, Figs 5 and 7 for a hollow cylindrical geometry and $\beta = 1.5$). The results in Figs 4-6 reveal similar dependencies of the transfer rate on β among the different geometries, i.e., the larger the geometry-dependent mass transfer rates along the
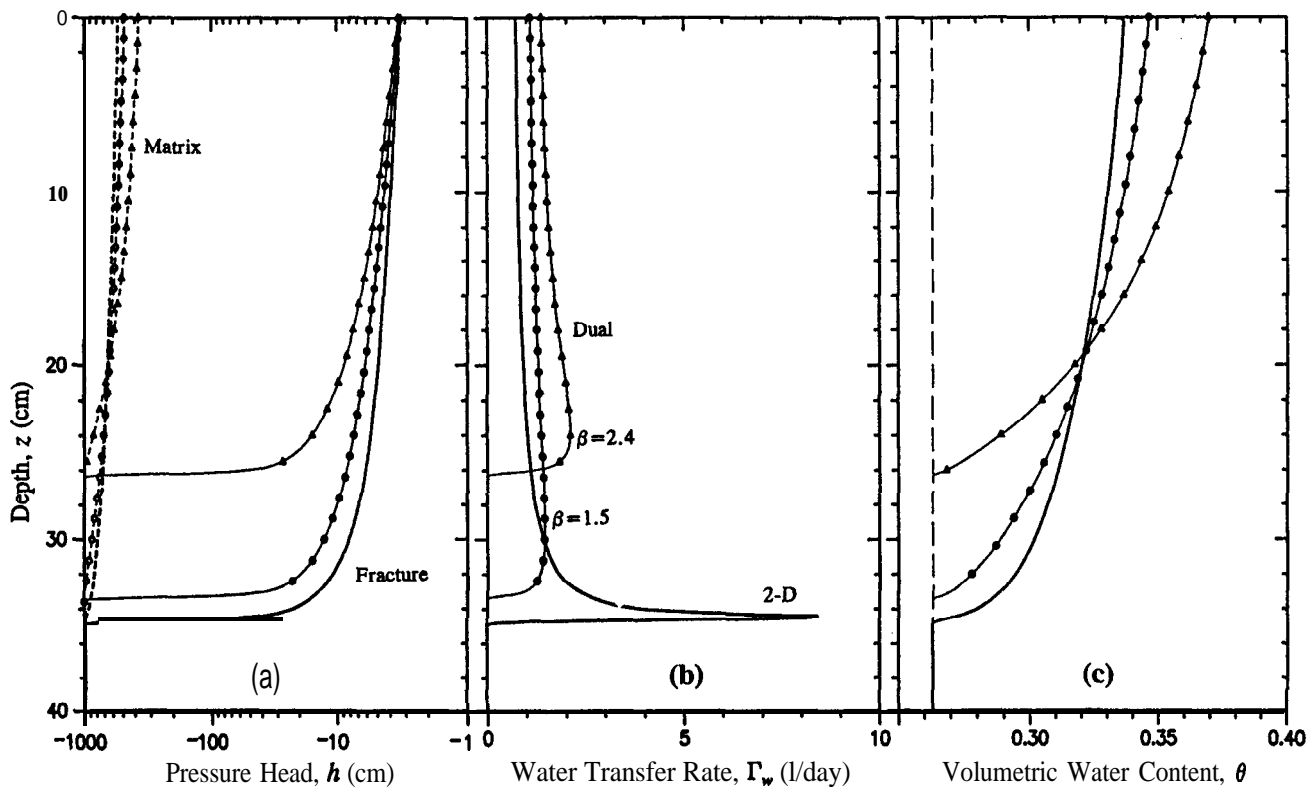

Fig. 5. Pressure head, h (a), water transfer rate, Γ_w (b), and total volumetric water content, θ (c), versus depth, z, at $t = 0.04$ days as calculated with the one-dimensional dual-porosity (Dual) and two-dimensional (2-D) models, assuming a hollow cylindrical geometry and relatively small water transfer rates ($K_{s,a} = 0.01$ cm/day); results are for geometry coefficients derived analytically ($\beta = 2.4$) and by direct matching ($\beta = 1.5$).

sequence: 'hollow cylinders < rectangular slabs < solid cylinders', the closer the match with the reference results. Thus, the closest correspondence was obtained for the solid cylindrical geometry (Fig. 6) assuming $\beta = 8$

In contrast to the above, the analysis becomes more complicated when, for a particular geometry, different methods for evaluating the geometry coefficient, β, are compared. Because of the approximate nature of the first-order approach, and the nonlinear flow regimes involved, the comparisons will differ for each particular set of hydraulic parameters and at each particular simulation time. We again present results at $t = 0.04$ for an infiltration event, and selected a situation with fairly typical results. In case of a hollow cylindrical geometry (Figs 5 and 7), the geometry coefficient obtained by direct matching, i.e., $\beta = 1.5$ calculated using (23), substantially improved the correspondence with the two-dimensional reference results, as compared to the analytically derived value ($\beta = 2.42$) using eqn (13). These results confirm that eqn (13) is limited to dual-porosity systems with relatively large values of ζ_0. On the other hand, results obtained with different values of β (as estimated analytically or using direct matching) were quite similar for rectangular slabs (Fig. 4), whereas for solid cylinders the results using the analytically derived

value turned out to be superior as compared to the direct matching method (Fig. 6). The results in Figs 4-6 only in part reflect the different sensitivities of the mass transfer rate on β for different matrix geometries. The results also support the assumption that a single constant value of 0.4 for the scaling coefficient, γ_w, in eqn (4) in combination with an arithmetically averaged K_a (eqn (5)) can be reasonably well applied to all three geometries.

EXTENSION TO MEDIA WITH COMPLEX STRUCTURAL GEOMETRIES

To be able to extend the approach to porous media with more complex structural geometries, we assume that somehow a macroscopic geometry-dependent coefficient may be defined which effectively captures the overall diffusion properties of the structured system. So far, β in eqn (4) was quantitatively related to the shape of a well-defined matrix structure. Alternatively, β could be related also to the ratio between the surface area of the interface between the fracture and matrix pore system and the volume of the matrix blocks. Both of these quantities are, at least in principle, measurable. The surface-to-volume ratio has been used in various
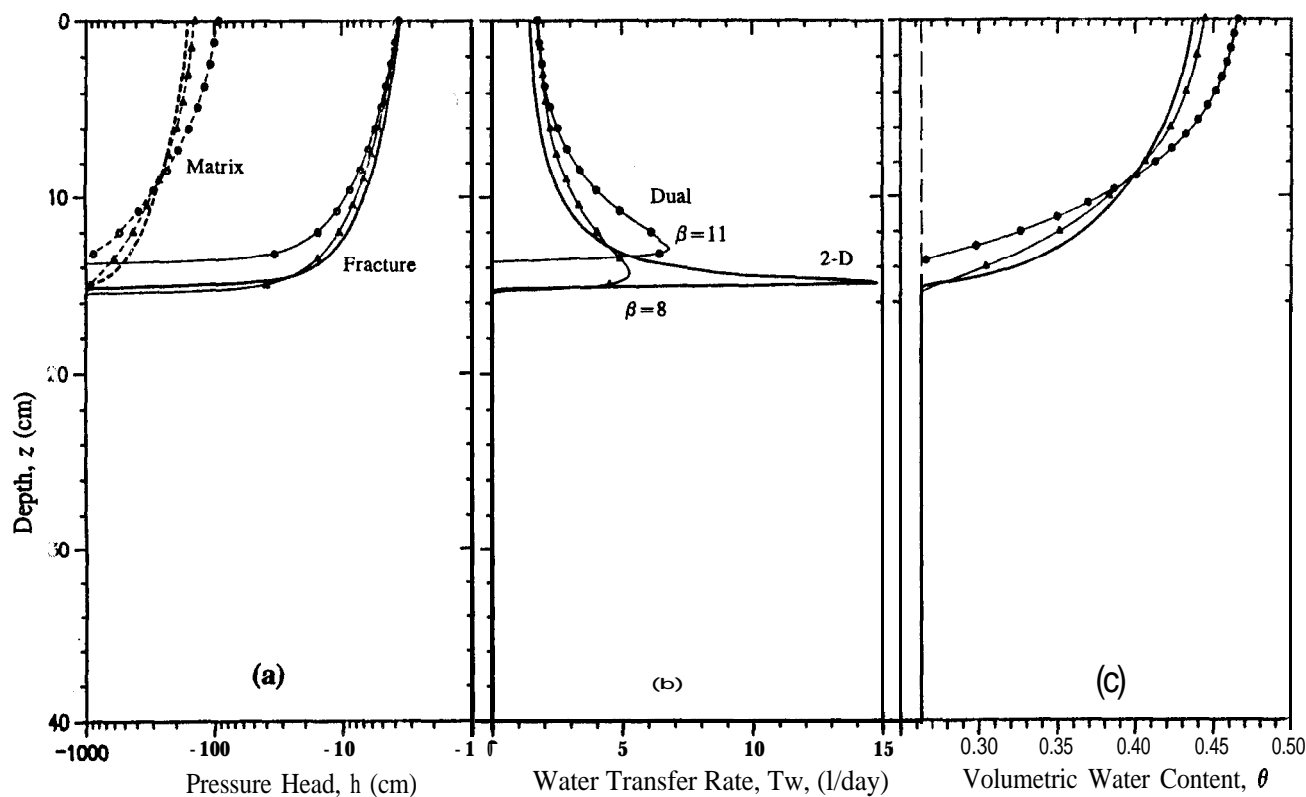

Fig. 6. Pressure head, h (a), water transfer rate, Γ_w (b), and total volumetric water content, θ (c), versus depth, z, at $t = 0.04$ days as calculated with the one-dimensional dual-porosity (Dual) and two-dimensional (2-D) models, assuming a solid cylindrical geometry and relatively small water transfer rates ($K_{s,a} = 0.01$ cm/day); results are for geometry coefficients derived analytically ($\beta = 8$) and by direct matching ($\beta = 11$).

approaches to obtain geometric information of soil or rock **structures,**[29,33,54] mostly from microscopic points of view.

The ratio between the surface area, A, (L^2), of the matrix-fracture interface (e.g., the soil aggregate surface) and the volume, V_m (L^3), in the case of a matrix block formed by parallel rectangular slabs (plates), is given by

$$\frac{A_{m,l}}{V_m} = \frac{1}{a_l} \tag{31}$$

which assumes that the contributions of the sides (top and bottom ends) can be ignored. For solid cylinders and rectangular prisms we obtain similarly

$$\frac{A_{m,c;m,r}}{V_m} = \frac{2}{a_{c;r}} \tag{32}$$

while for spheres the surface-area-to-volume ratio is

$$\frac{A_{m,s}}{V_m} = \frac{3}{a_s} \tag{33}$$

For hollow cylinders, assuming that water and solute mass transfer is restricted to the surface area of the inner cylinder, one obtains

$$\frac{A_{m,h}}{V_m} = \frac{2}{b_h(\zeta_0^2 - 1)} = \frac{2}{a_h(\zeta_0 + 1)}; \qquad \zeta_0 > 1 \tag{34}$$

where $a_h = b_h(\zeta_0 - 1)$ is the characteristic length of the matrix structure.

For application to media with arbitrary geometries and various characteristic diffusion lengths, we introduce a dimensionless surface-area-to-volume ratio, $\varsigma(-)$, normalized per unit length of the matrix structure for rectangular and solid cylindrical geometry

$$\varsigma = \frac{A_m^*}{V_m} a^* \tag{35}$$

and for hollow cylindrical structures

$$\varsigma = \frac{2}{(\zeta_0 + 1)}; \qquad \zeta_0 > 1 \tag{36}$$

where A_m^* is the effective surface area and a^* is the effective length of the matrix pore system, both being lumped macroscopic scale parameters which integrate over all geometries of a defined volume of the structured medium.

By assuming lumped parameters, we may plot the geometry coefficient, β, versus the normalized surface-area-to-matrix-volume ratio, ς, obtained from the directly-matched shape factors for various sizes and shapes for conversion into the equivalent first-order rate model using eqn (22). Results are shown in Fig. 8 where, for comparison, the analytically-derived coefficients for
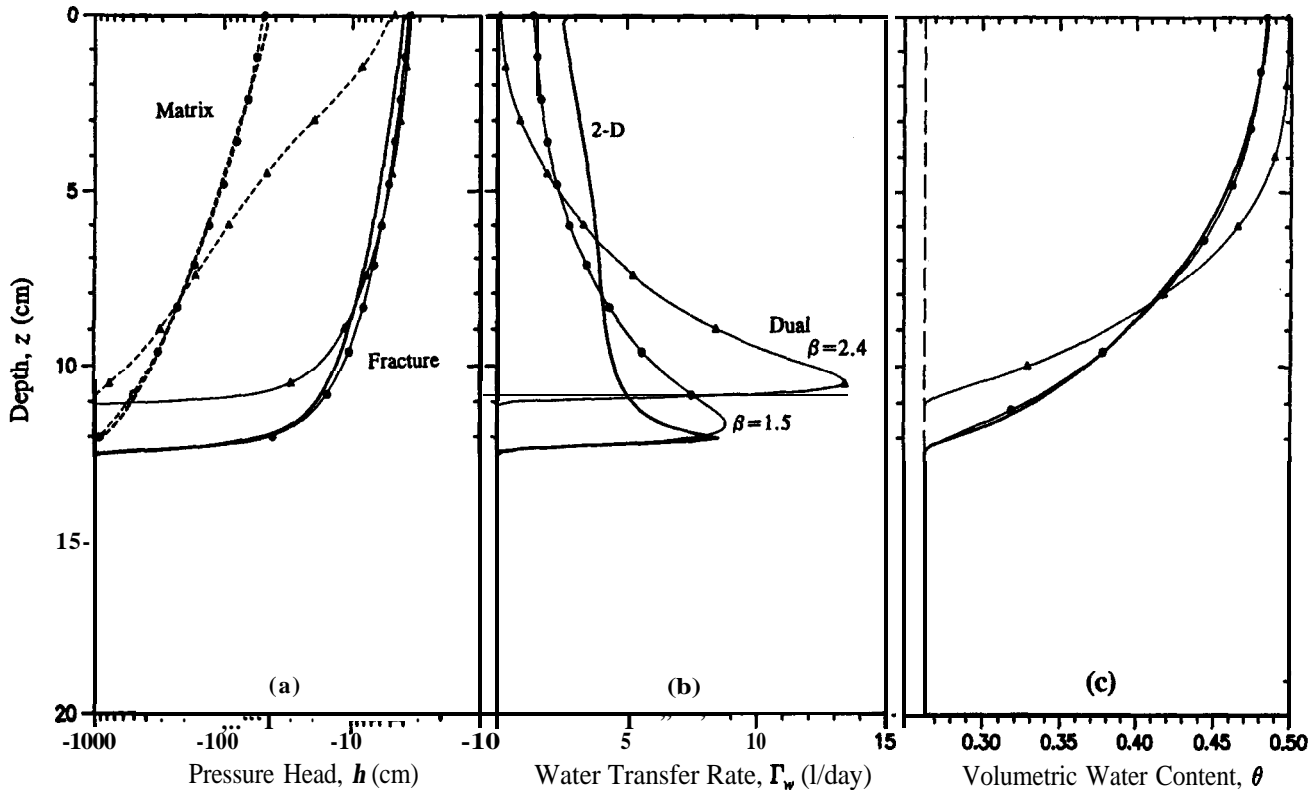

Fig. 7. Pressure head, *h* (a), water transfer rate, Γ_w (b), and total volumetric water content, θ (c), versus depth, *z*, at *t* = 0·04 days as calculated with the one-dimensional dual-porosity (Dual) and two-dimensional (2-D) models, assuming a hollow cylindrical geometry and relatively large water transfer rates ($K_{s,a}$ = 0·1 cm/day); results are for geometry coefficients derived analytically (β = 2.4) and by direct matching (β = 1·5).

plane sheets, solid cylinders, and spheres have been included. Figure 8 shows that the difference in the value of β between structures that have the same reduced surface-to-volume ratio, are much smaller than differences in β with respect to the method of evaluation (e.g., $\beta = 22.7$ for a sphere and 20.7 for a cube). This fact permits one to describe the geometry coefficient over a wide range of c-values by the fitted empirical expression

$$\beta = \begin{cases} \left[0.19\ln\left\{16\left(\frac{2}{\varsigma}-1\right)\right\}\right]^{-2} & 0.0198 < \varsigma < 1 \\ 3.6\varsigma^{1.5} & 1 \le \varsigma \le 2 \\ u_1 + u_2\varsigma + u_3\varsigma^2 & 2 < \varsigma \le 10 \end{cases} \tag{37}$$

in which $u_1 = 11.4275$, $u_2 = -7.4438$, and $u_3 = 3.5473$ and where $r^2 = 1$. For $1 < \varsigma < 2$, the appropriate geometry coefficients may be obtained by using the interpolation function suggested in eqn (37). Alternatively. the dependency may be described also by

$$\beta = \begin{cases} \left[0.19\ln\left\{16\left(\frac{2}{\varsigma}-1\right)\right\}\right]^{-2} & 0.0198 < \varsigma < 1 \\ \left[\dfrac{0.65}{0.09+\varsigma}\right]^{-2} & 1 \le \varsigma \le 10 \end{cases} \tag{38}$$

which is simpler but also somewhat less accurate than eqn (37).

The proposed functions in eqns (37) or (38) relate the geometry-dependent coefficient, β, of the macroscopic scale mass transfer terms in eqn (12) to macroscale properties of an arbitrarily structured medium. The functional interpretation of structure used here focuses only on the size and shape of the fracture-matrix interface area through which diffusive mass transfer actually takes place. An important lumped parameter in this context is the effective surface area, A_m^*, which integrates all 'internal' structural surfaces over the volume of the porous medium; its value also contains contributions from imperfectly developed (sub-) structures such as small fissures in spherical or cylindrical matrix blocks. Values of the normalized surface-area-to-volume ratio smaller than unity represent structured soils or fractured rocks in which the 'internal' surface area for diffusive mass transfer is primarily concave (e.g., hollow cylinders). For porous media having values of $\varsigma > 1$, the fracture-matrix interface areas are predominantly convex (e.g., spheres). The effective characteristic length parameter, a^*, may be interpreted to be the smallest average distance for diffusion between the
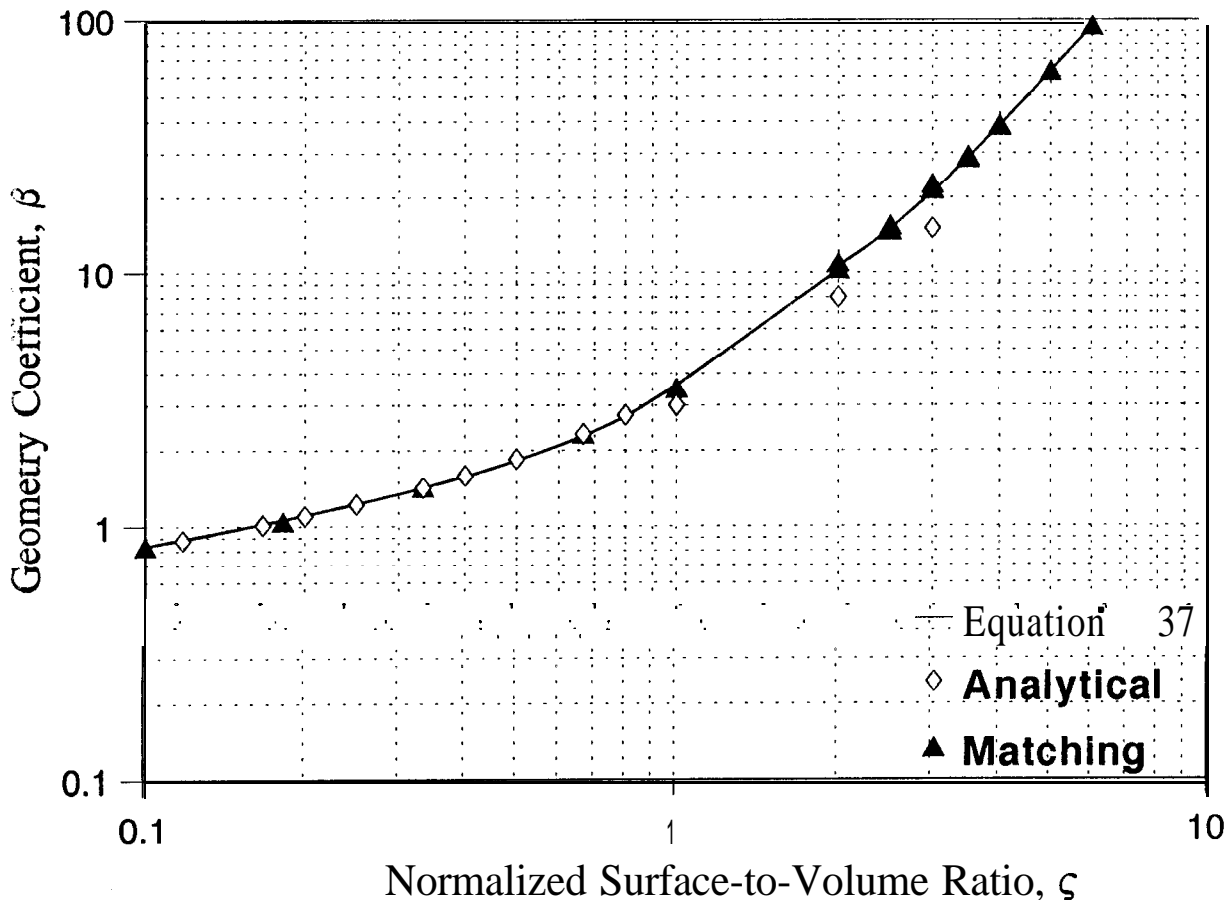

Fig. 8. Plot of the geometry coefficient β as a function of the normalized effective surface-to-volume ratio, $\varsigma = a^* A_m^*/V_m$, as given by eqn (37), as well as p-values obtained by analytical evaluation and direct matching.

fracture-matrix interface and the center of the matrix blocks perpendicular to the macroscopic scale flow direction. The results in Fig. 8 suggest that the effect of β on flow and transport calculations will be most apparent when ς is close to $1 \cdot 0$. The effect of β declines for $\varsigma \ll 1$ where β approaches a relatively constant value of $0 \cdot 5$ (i.e., the asymptotic behavior of β for $\varsigma < 0 \cdot 1$ is demonstrated in Fig. 2) and total mass transfer rates decrease because of a reduced effective surface area for transfer, A_{m}^{*}. For $\varsigma \gg 1$, the effect of β may also decline if, in the case of relatively large mass transfer rates, the situation of a homogeneous (unstructured) medium is approached which will not exhibit any preferential flow. We emphasize that the coefficient β as estimated with eqn (37) or eqn (38) accounts for the shape dependency of the mass transfer process, and indirectly still is a function of the characteristic length, a^{*}. The macroscale parameters a^{*}, b^{*}, and w_{f}, however, are no longer related to each other in well-defined ways as for idealized geometries using eqns (31)-(34); they have to be measured independently.

POSSIBLE PARAMETERIZATION OF STRUCTURAL GEOMETRY

Most approaches involving microstructure-type mobile-immobile models assume prior knowledge of the type of geometry, or rely on detailed micromorphological measurements.[29,32,33,54] In addition, an equivalent dia-meter concept has been proposed for tubular macropores in saturated media.[12] However, we believe that realistic simulations of preferential flow require the use of macroscopic scale flow and transport parameters for both pore systems.

The macroscopic approach presented in this paper permits structural effects to be included without assum-ing any type of geometry *a priori,* and hence follows a more functional view as suggested previously by Bouma *et al.*[7] The proposed macroscopic scale representation of the structural geometry leading to diffusive mass transfer relies on one of the most basic properties of a structured medium, i.e., the fracture-matrix interface area. The extent, size and shape of the interface, as well as its physical, chemical, and biological properties (e.g., those of fracture coatings) are major factors determining transport processes in aggregated soils or fractured rocks. Of relevance here are, as discussed earlier,[16] not only the interfacial permeability, K_{a}, but also the effective diffusion coefficient, D_{a}, the chemical composi-tion and sorption sites, biological activities along fractures, as well as other properties occurring at or near such interfaces.

Unfortunately, the effective fracture-matrix interface area is not easily determined experimentally. Under certain conditions the area and shape of the interface may actually depend on the water content and flow rate,

while also partial wetting of aggregate surfaces or swelling and shrinking of the matrix may occur. Recently, methods have been suggested to calculate the surface areas of structured soils using dyes that stain macropore **areas**[5,18] or by using an image **analyzer.**[6] Measurements of air permeability have also been **suggested**[36] to determine the effects of pore geometry on transport processes in macroporous soils. Birgersson *et al.*' used two different tracers at the same time to estimate the flow-wetted surface of fractured rocks into which the dyes can diffuse and sorb. In another study, McKay *et al.*[26] used nonreactive solute and colloid-sized bacteriophage tracers to reveal large differences in trans-port rates between the two tracers because of exclusion of the large tracers from diffusing into the matrix.

The second macroscopic property, the effective characteristic length of the matrix structure, a^{*}, may be determined using diffusion experiments. As a reason-able initial estimate for a^{*}, one-half of the volume-surface mean diameter d (as defined by Gregg and Sing") may be used:

$$a^{*} = \frac{d_{\mathrm{V,A}}}{2} = \frac{1}{2} \frac{\sum(n_i l_i^3)}{\sum(n_i l_i^2)} \tag{39}$$

where n_i are the number of particles (cubes) of edge length l_i of a specific volume. Often, the values of the lengths l_i in eqn (39) have to be estimated, for example, by using the mean projected diameter," which is the diameter of a circle having the same area as the projected image of the particle when viewed in a direction normal to the plane of greatest stability. One could apply a similar approach to aggregate mixtures so as to obtain a weighted average of the geometry and length coefficient. Mass transfer rates could also be obtained by multiple calculations using observed shape and size distributions of the matrix pore system, and applying a volumetric weighing procedure.

The above modeling concept offers also the possibility to combine mass transfer with preferential flow in situations involving partial wetting of matrix surfaces of cracked clays or fractured rocks, for instance, by assuming

$$A_{\mathrm{m}}^{*} = A_{\mathrm{m}} s, \qquad 0 \leq s \leq 1 \tag{40}$$

where $s(t)$ is a dimensionless wetting parameter which may be a function of time or certain soil **properties.**[21] The effects of swelling and shrinking in soils in this approach could be described directly by means of the parameter w_{f}.

CONCLUSIONS

Preferential flow of water in a dual-porosity system of various matrix geometries was simulated using a first-order type water transfer term. Direct comparisons with

reference two-dimensional model simulations demonstrate (1) inherent limitations in the approach because of simplification of highly nonlinear transfer processes into an approximate first-order rate model, and (2) sensitivity of the mass transfer coefficient in the dual-porosity model to the exact geometry of the matrix pore system (e.g., rectangular slabs, and hollow or solid cylinders). The comparisons revealed similar tendencies for all three geometries when using an appropriate value of the coefficient, β, describing the specific geometry of the matrix pore system. By scaling the diffusion properties and relating the geometry coefficient to the ratio between effective surface area at the fracture-matrix interface and matrix volume, the approach may be extended to media with arbitrary and complex internal geometries.

The methodology in this paper gives qualitatively a good approximation of more realistic two-dimensional representations of the mass transfer process. An important advantage of the scaling approach is that the method can be readily incorporated in multi-dimensional numerical models (e.g., Vogel et *al.*[48]). Also, the model may be used as a tool to represent or better understand preferential flow and transport phenomena in a mechanistic (process-based) fashion with a reasonable numerical effort. The approach enhances the utility of dual-porosity models in that otherwise empirical fitting parameters now can be expressed in terms of measurable soil/rock properties. Also, the approach is shown to be not limited to porous media containing a single type of aggregate shape and size (geometry) or uniformly-sized aggregates, nor is an a *priori* qualitative description of the geometry of the porous matrix required. The approach is also not limited to experimentally determined aggregate size distributions, which often are difficult to obtain for specific soils. Nevertheless, the study of interfacial macroscale properties will require new or improved experimental methods for determining effective surface areas, i.e., those of soil aggregates or fracture walls. The approach may help to further increase the applicability of the dual-porosity approach to analyze transport in media with complex and widely-differing structural geometries.

REFERENCES

1. Barenblatt, G. I., Zheltov, I. P. & Kochina, I. N., Basic concepts in the theory of seepage of homogeneous liquids in fissured rocks. *J. Appl. Math. Mech. Engl. Transl., 24* (1960) 1286-1303.
2. Barker, J. A., Block-geometry functions characterizing transport in densely fissured media. *J. Hydrol., 77* (1985) 263-279.
3. Birgersson, L., Moreno, L., Neretnieks, I., Widen, H. & Agren, T., A Tracer Migration Experiment in a small fracture zone in granite. *Water Resour. Res., 29* (1993) *3867-3878.*
4. Bolt, G. H., Movement of solutes in soil: Principles of adsorption/exchange chromatography. In *Soil Chemistry, B. Physico-Chemical Models, Dev. Soil Sci. 5B,* ed. G. H. Bolt, 1979, pp. 295-348.
5. Booltink, H. W. G. & Bouma, J., Physical and morphological characterization of bypass flow in a well-structured clay soil. *Soil Sci. Soc. Am. J., 55 (1991) 1249-1254.*
6. Booltink, H. W. G., Hatano, R. & Bouma, J., Measurement and simulation of bypass flow in a structured clay soil: A physico-morphological approach., *J. Hydrol., 148* (1993) 149-168.
7. Bouma, J., Belmans, C. F. M. & Dekker, L. W., Water infiltration and redistribution in a silt loam subsoil with vertical worm channels. *Soil Sci. Soc. Am. J., 46* (1992) 917-921.
8. Brusseau. M. L. & Rao. P. S. C.. Modeling solute transport in structured soils: A review. *Geoderma, 46* (1990) 169-192.
9. Carslaw, H. S. & Jaeger, J. C., *Conduction of Heat in Solids,* 2nd edition. Oxford University Press, London, 1959.
10. Coats, K. H. & Smith, B. D., Dead end pore volume and dispersion in porous media. Soc. *Petrol. Eng. J., 4 (1964) 73-84.*
11. Crank, J., The *Mathematics of Diffusion.* Oxford Uuiversity Press, London, 1956, 347 pp.
12. Dunn, G. H. & Phillips, R. E., Equivalent diameter of simulated macropore systems during saturated flow. *Soil Sci. Soc. Am. J., 55* (1991) 1244-1248.
13. Dykhuizen, R. C., Transport of solutes through unsaturated fractured media. *Water Res., 21* (1987) 1531-1539.
14. Dykhuizen, R. C., A new coupling term for double-porosity models. *Water Resour. Res., 26 (1990) 351-356.*
15. Gerke, II. H. & van Genuchten, M. T., A dual-porosity model for simulating the preferential movement of water and solutes in structured porous media. *Water Resour. Res., 29* (1993), 305-319.
16. Gerke, H. H. & van Genuchten, M. T., Evaluation of a first-order water transfer term for variably-saturated dual-porosity models. *Water Resour. Res., 29* (1993) 1225-1238.
17. Gish, T. J. & Shirmohammadi, A.(eds.), *Preferential flow.* Proceedings of the national symposium, 16- 17 December 1991, Chicago, Illinois, American Society of Agricultural Engineers, St. Joseph, Michigan, 1991, 408 pp.
18. Ghodrati, M. & Jury, W. A., A field study using dyes to characterize preferential flow of water. *Soil Sci. Soc. Am. J., 54 (1990) 1558-1563.*
19. Gregg, S. J. & Sing, K. S. W., *Adsorption, Surface Area and Porosity,* 2nd edition. Academic Press, London, 1982.
20. Heijs, A. W. J., de Lange, J., Schoute, J. F. T. & Bouma, J., Computed tomography as a tool for non-destructive analysis of flow patterns in macroporous clay soils. *Geoderma, 64* (1995) 183-196.
21. Hoogmoed, W. B. & Bouma, J., A simulation model for predicting infiltration into cracked clay soil. *Soil Sci. Soc. Am. J., 44* (1980) 458-461.
22. Hornung, U., Homogenization of miscible displacement in unsaturated aggregated soils. In Workshop on Composite Media and Homogenization Theory, ICTP, Tricste, 1990, *Progress in Nonlinear Differential Equations and Applications,* eds., DalMaso, G. & Dell'Antonio, G. F. Birkhäuser, Boston, 1991, pp. 143-153.
23. Hornung, U. & Showalter, R. E., Diffusion models for fractured media. *J. Math. Anal. Appl., 147 (1990) 69--80.*
24. Jarvis, N. J., Jansson, P.-E., Dik, P. E. & Messing, I., Modelling water and solute transport in macroporous soil. I. Model description and sensitivity analysis. *J. Soil Sci.,* 42 (1991) 59-70.

25. Joschko, M., Graff, O., Muller, P. C., Kotzke, K., Lindner, P., Pretschner, D. P. & Larink, O., A non-destructive method for the morphological assessment of earthworm burrow systems in three dimensions by X-ray computed tomography. *Biol. Fertil. Soils,* 11(199 1) *88-92.*

26. McKay, L. D., Gilham, R. W. & Cherry, J. A., Field experiment in a fractured clay till. *Water Resour. Res., 29 (1993) 3879-3890.*

27. Moldrup, P., Rolston, D. E., Hansen, J. A. & Yamaguchi, T., A simple, mechanistic model for soil resistance to plant water uptake. *Soil Sci.,* 153 (1992) 87-93.

28. Molz, F. J., Models of water transport in the soil-plant system: A review. *Water Resour. Res., 17 (1981) 1245-1260.*

29. Neretnieks, I. & Rasmuson, A., An approach to modelling radionuclide migration in a medium with strongly varying velocity and block sizes along the flow path. *Water Resour. Res., 20 (1984) 1823-1836.*

30. Parker, J. C. & Valocchi, A. J., Constraints on the validity of equilibrium and first-order kinetic transport models in structured soils. *Water Resour. Res., 22 (1986) 399-407.*

31. Raats, P. A. C., Transport in structured porous media. *Proc. Euromech. (Delft), 143 (198 1) 221-226.*

32. Rao, P. S. C., Jessup, R. E. & Addison, T. M., Experimental and theoretical aspects of solute diffusion in spherical and non-spherical aggregates. *Soil Sci.,* 133 (1982) 342-349.

33. Rappoldt, C., The application of diffusion *models* to an aggregated soil. *Soil Sci.,* 150 (1990) 645-661.

34. Rasmuson, A. & Neretnieks, I., Exact solution for diffusion in particles and longitudinal dispersion in packed beds. *J. Am. Inst.* Chem. *Eng.,* 26 (1980) 686-690.

35. Rasmuson, A., Gimmi, T. & Flühler, H., Modeling reactive gas uptake, transport, and transformation in aggregated soils. *Soil Sci. Soc. Am. J., 54 (1990) 1206-1213.*

36. Roseberg, R. J. & McCoy, E. L., Measurement of soil macropore air permeability. *Soil Sci. Soc. Am. J., 54 (1990) 969-974.*

37. Simunek, J., Vogel, T. N. & van Genuchten, M. T., The SWMS_2D code for simulating water flow and solute transport in two-dimensional variably-saturated media, Research Report No. 126, U. S. Salinity Laboratory, USDA, ARS, Riverside, CA, 1992.

38. Skopp, J., Gardner, W. R. & Tyler, E. J., Miscible displacement in structured soils: Two region model with small interaction. *Soil Sci. Soc. Am. J., 45* (1981) 837-842.

39. Sudicky, E. A., The Laplace Transform Galerkin Technique for efficient time-continuous solution of solute transport in double-porosity media. *Geoderma, 46 (1990) 209-232.*

40. Valocchi, A. J., Use of temporal moment analysis to study reactive solute transport in aggregated porous media. *Geoderma, 46 (1990) 233-247.*

41. van Genuchten, M. T., A general approach for modeling solute transport in structured soils. *Memoires Znt. Assoc. Hydrogeol., 17 (1985)* 513-526.

42. van Genuchten, M. T., New issues and challenges in soil physics research, Transactions, 15th World Congress of Soil Science, Acapulco, Mexico, July 10-16, 1994, Volume 1, 5-27, Int. Soc. of Soil Sci. and Mexican Soc. of Soil Sci., 1994.

43. van Genuchten, M. T. & Wierenga, P. J., Mass transfer studies in sorbing porous media. I. Analytical Solutions. *Soil Sci. Soc. Am. J., 40 (1976) 473-480.*

44. van Genuchten, M. T. & Dalton, F. N., Models for simulating salt movement in aggregated field soils. *Geoderma, 38 (1986) 165-183.*

45. van Genuchten, M. T. & Gerke, H. H., Dual-porosity models for simulating solute transport in structured media, Proceedings, Colloquium 'Porous or Fractured Unsaturated Media: Transports and Behaviour', October 5-9, 1992, Monte Verita, Ascona, Switzerland, 1993, pp. 182-205.

46. van Genuchten, M. T., Tang, D. H. & Guennelon, R., Some exact and approximate solutions for solute transport through soils containing large cylindrical macropores. *Water. Resour. Res., 20 (1984) 335-346.*

47. van Genuchten, M. T., Leij, F. J. & Yates, S. R., The RETC-code for quantifying the hydraulic functions of unsaturated soils, Report EPA/600/2-91/065, Washington, DC, 1991.

48. Vogel, T. N., Zhang, R., Gerke, H. H. & van Genuchten, M. T., Modeling two-dimensional water flow and solute transport in heterogeneous soil systems. In *Hydrologic Investigation, Evaluation, and Ground Water Modeling,* eds. Y. Eckstein & A. Zaporozec. Proceedings of Industrial and Agricultural Impacts on the Hydrologic Environment, The Second USA/CIS Joint Conference on Environmental Hydrology and Hydrogeology, 16-21 May 1993, Washington, D. C., 1993, pp. 279-302.

49. Wang, J. S. Y., Flow and transport in fractured rocks. *Reviews* Of Geophysics, Supplement (1991) 254-262.

50. Warner, G. S., Nieber, J. L., Moore, I. D. & Geise, R. A., Characterizing macropores in soil by computed tomography. *Soil Sci. Soc. Am. J.,* 53 (1989) 653-660.

51. Warren, J. E. & Root, P. J., The behaviour of naturally fractured reservoirs. Soc. *Petrol. Eng. J., 3 (1963) 245-255.*

52. Zimmerman, R. W. & Bodvarsson, G. S., Integral method solution for diffusion into a spherical block. J. *Hydrol.,* 111 (1989) 213-224.

53. Zimmerman, R. W. & Bodvarsson, G. S., An approximate solution for one-dimensional absorption in unsaturated porous media. *Water Resour. Res., 25 (1989) 1422-1428.*

54. Zimmerman, R. W., Bodvarsson, G. S. & Kwicklis, E. M., Adsorption of water into porous blocks of various shapes and sizes. *Water Resour. Res., 26 (1990) 2797-2806.*

55. Zimmerman, R. W., Chen, G., Hadgu, T. & Bodvarsson, G. S., A numerical dual-porosity model with semianalytical treatment of fracture/matrix flow. *Water Resour. Res., 29 (1993) 2127-2137.*